AN ANALYSIS OF MOLDING AND CURING OF SMC BY THE FINITE ELEMENT METHOD

Naksoo Kim

Department Mechanical Engineering, Hong-Ik University

Abstract

A thermo-viscoplastic finite element program was developed to analyze the compression molding of SMC process. Deformation of the material was modelled by using the flow-rule. Heat balance during the process was coupled to the deformation. In the cure study, a kinetic model was adopted to describe the cure behaviour. The numerical kinetic model was integrated with the thermo-viscoplastic numerical analysis by adding heat generation due to the chemical reaction of the workpiece in the heat transfer analysis. The integrated finite element program can simulate a whole sequential molding process including deformation, heat transfer, and chemical reaction. A practical SMC molding process with T-shaped substructure was simulated. The simulated results showed good agreements with experiments.

I. INTRODUCTION

Compression molding is used in the fabrication of SMC(Sheet Molding Compound) into desired shapes. Cross-linking is completed in the heated die, with curing times ranging from 0.5min to 5min, depending on the material and part geometry. The process of compression molding of SMC normally involves mold filling, curing, ejection of parts and cool-down as schematically shown in Fig. 1. Product quality and production rate are determined by die design, temperature, pressure, and cycle time. In SMC molding, many serious problems often occur around the intersections of the main part and the substructures. For example, the fibers distribute nonuniformly as illustrated in Fig. 2 and a sink mark frequently develops on the top surface mainly due to the material nonuniformity and the shrinkage during the cooling stage.

Most analyses of SMC curing assume that the mold is filled with SMC before any heat transfer and reaction occurs. In the actual SMC compression molding, material flow starts as the charge is placed on the bottom mold. The top mold moves down rapidly until it nearly touches the charge surface in order to reduce heat conduction between the charge and the bottom mold. Heat conduction during this stage, called

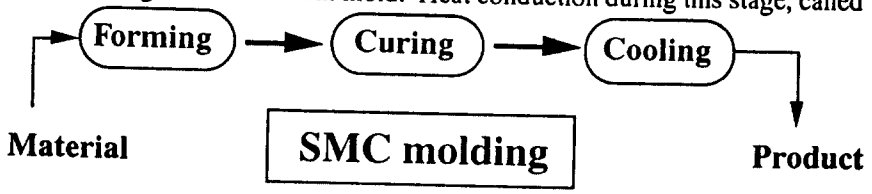

Fig. 1 Sheet Molding Compound Forming.

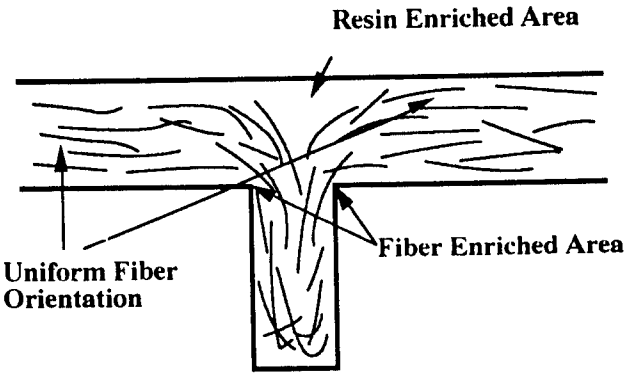

Fig. 2 Fiber distributions and mechanics of sink formation.

dwelling, leads to a non-isothermal and asymmetric flow with respect to the midplane of the charge. This may generate an asymmetric temperature profile and non-uniform distributions of curing agents (i.e., inhibitor and initiator) concentration through the SMC part, which may result in a non-uniform curing pattern, or so called "dwelling effect".

Due to the complexity resulting from the interaction among mold filling, heat transfer, and cure reaction, it is not easy to analyze the entire process as a whole. During mold filling, heat transfer from the mold to the charge may result in a non-uniform temperature distribution which in turn may generate a non-uniform consumption of inhibitors at different locations. This can be readily analyzed by incorporating the decomposition rate of curing agents in the flow simulation and calculating the distributions of temperature and curing agents concentration during mold filling.

In this study, the mold filling and curing stages are discussed. A numerical analysis of compression molding at non-isothermal conditions was carried out to investigate the SMC flow under various processing conditions in molds with substructures. The concentration of curing agent at different locations will be affected by the flow and heat transfer. In the cure simulation, a kinetic model found in the literature was adopted to describe the cure behavior, which was then combined with a heat transfer model to simulate the SMC cure by the use of a finite element program.

II. REVIEW OF PREVIOUS WORKS

II.1 Flow Study of SMC

Many researchers have used a squeeze flow rheometer to characterize the flow properties of SMC under compression molding.[1,2] Lee, et al.[3] modelled the SMC flow by shear and elongational deformation by assessing two different friction conditions at the mold-SMC interface. A model which considered SMC as a Newtonian

fluid with a transverse viscosity gradient was proposed by Lee, et al.[4] Barone and Caulk[5] and Castro[6] modelled the SMC flow as a combination of an in-plane extensional resistance due to fiber-resin interaction and a friction response at the mold interface. All of these research works are limited to the flow over planar geometries.

Experimentally, mold filling of SMC has been studied by many researchers. Marker and Ford[7] performed the compression molding by using color-layered charges and pointed out that during molding the hotter, low viscosity surface layers acted as a lubricant and the cooler central layers underwent an equal biaxial extensional deformation, which resulted in a differential shrinkage during molding, a non-uniform pressure pattern, and frozen residual stresses in the cured part. Barone and Caulk[8] demonstrated that flow would affect the fiber orientation and consequently the final mechanical property and cosmetic appearance. A flow visualization study of SMC using carbon black tracers, which provided a semi-quantitative description of the flow, was conducted by Kau [9].

Efforts have also been contributed to the simulation of SMC flow. Silva-Neito, et al.[10] applied an isothermal Newtonian model to predict the SMC flow. Tucker and Folgar[11] used the Hele-Shaw's flow model and a finite element method to simulate the flow front propagation of a rectangular charge under compression. Lee and Tucker[12] proposed a simple model using a two-dimensional finite element formulation for the flow in planar geometries based on the assumption of an isothermal flow with a flat velocity profile. Osswald and Tucker[13] extended this model to 3-D. Although their model can predict the flow front progression of SMC in molds with complicated geometry, with the assumptions used, the molding pressure, the deformed shape of flow front, and the temperature field near the interface between the mold and the charge cannot be well determined.

For thermal analysis, Barone and Caulk[14] modelled heat transfer to the molding compound from the hot mold during the filling stage by assuming a plug type filling pattern. Lee and Tucker[15] considered the heat transfer effect by treating the charge as eight separate layers with different viscosities. Fan, et al.[16] studied the SMC flow using a squeeze flow rheometer to measure the flow resistance under compression. Based on the experimental observation, they used a two-step approach to simulate the SMC flow in the T-shape mold. At the first step, the SMC charge was presumed to be compressed in a flat plate like mold configuration. A T-shape mold configuration replaced the flat plate mold when the pressure reached a critical value that SMC started to flow into the slot at the second step. The corresponding temperature contour at the end

of mold filling was used as the initial condition of SMC cure analysis by the finite difference method.

It should be noted that a realistic flow model should consider the anisotropic nature of the molding compound in the flow study of SMC. If an isotropic flow model is to be used, it has to be modified according to the actual flow pattern in the mold. Recently, Kim[17] studied the effects of anisotropy due to the inclusions of short-fibers in SMC, both experimentally and numerically.

II.2 Cure Study of SMC

The cure reaction of SMC is basically a radical chain growth copolymerization between the styrene monomer and the unsaturated polyester molecule. Stevenson [18] and Lee [19] developed a series of kinetic models for unsaturated polyester resins based on the usually accepted reaction mechanism of free radical copolymerizations. Unlike the empirical model proposed by Kamal et al.[20] , these mechanistic models not only provided the necessary kinetic information for the heat transfer modelling, but also elucidated the functions of initiators, inhibitors and monomers in the reaction up to the medium conversion region.

Cure analysis of SMC molding has been carried out by several researchers either experimentally or theoretically. Herman[21] investigated the heat flow during SMC molding and proposed a method for designing an appropriate mold heating system. Mallick and Raghupathi[22] studied the effect of cure cycle on mechanical properties, and suggested that preheating would offer advantages of reducing both the mold cycle time and the thermal gradient. Stevenson[23] applied their kinetic models to investigate the SMC cure during compression molding. Lee[24] applied the same model to analyze the reaction profiles in molds with different geometries using a finite element method. In his analysis, the mold filling stage was ignored and the temperature of the charge was assumed to be at room temperature when the cure reaction started.

Although the individual applications of a FEM program to mold filling and a FDM program to curing have demonstrated to be useful for process analysis of SMC molding in molds with substructures[16], it is limited to parts with simple geometries because of the FDM formulation. It would be desirable that the reaction term can be incorporated into the FEM formulation such that the analysis can be applied to various compounds and mold geometry without any limitation.

III. THEORETICAL KINETIC MODELLING

III.1 Kinetic model

Since SMC resins gel at very low conversions, a premature gelling may occur if the curing reaction starts during mold filling. This may result in scorch problem, or a poor surface finish of molded parts and cause incomplete filling. Therefore, a SMC compound must be designed in such way that no cure reaction occur during mold filling. This is achieved by controlling the type and concentration of initiators and inhibitors in the curing agents. Inhibitors are capable of preventing the cure reaction by reacting with free radicals generated in the system. They provide an induction time for the compound to fill the mold without any scorch problem. At higher temperatures, initiators are more active and can generate free radicals faster, therefore, the induction time will be shorter. For an ideal SMC compound, the induction time should be long enough to ensure complete mold filling, yet short enough to achieve a short cure time.

A kinetic model proposed by Stevenson[18] and Lee[19] was adopted in this study. Since the model was derived by considering the function of every major component in the SMC compound, it is useful for the cure analysis. The model assumed that the SMC reaction can be described as a combination of three steps: initiation, inhibition, and propagation. Reaction starts only after the number of initiator radicals created is equal to the effective number of inhibitor molecules initially presented. The governing equations of the kinetic mechanism can be written as follows.

Initiation:

$$\frac{dR\bullet}{dt} = 2k_d I \quad , \tag{1}$$

where k_d is initiator decomposition rate constant, I, the concentration of the initiator, and $R\bullet = 2f(I_r - I)$ was used, where I_r is the concentration of residual initiator after all the inhibitors having been consumed, and f, the initiator efficiency.

Inhibition:

$$qZ_o = 2fI_o(1 - e^{-\int_0^{t_z} k_d dt}) = 2f(I_o - I_r) \quad , \tag{2}$$

where I_o and Z_o are the initial concentrations of initiator and inhibitor, respectively, q, the inhibitor efficiency, and t_z, the induction time before propagation.

Propagation:

$$\frac{dM}{dt} = -k_p M R\bullet \tag{3}$$

or

$$\frac{d\alpha}{dt} = 2fI_r k_p (1-\alpha)(1 - e^{-\int_0^{t-t_z} k_d d(t-t_z)}) \quad , \tag{4}$$

where M is the monomer concentration, k_p, propagation rate constant, and α, the fractional conversion. The kinetic parameters, k_d and k_p, can be estimated from iso-

thermal DSC experiments. They are assumed to be Arrhenius temperature dependent throughout the entire cure, where

$$k_d = A_d \exp(-E_d/RT) \quad \text{and} \quad k_p = A_p \exp(-E_p/RT) \tag{5}$$

The induction time (or inhibition period) depends on the type and concentration of initiators and inhibitors. For an ideal compound, one would like to have a short cure time in order to reduce the production cycle, and a long enough induction time in order to prevent the scorch problem. Increasing the cure temperature reduces both the induction time and the cure time. This indicates that changing the temperature only is insufficient in obtaining an optimal molding.

III.2 Numerical procedure

Heat is generated by the chemical reaction during the curing process. The information on the distributions of the ongoing chemical reaction-related variables are important to expect the material properties of the product. The effect of the chemical reaction cannot be underestimated when it happens during the forming process. By using the chemical reaction model suggested by other researchers, a useful FEM code to simulate forming and curing processes of polymers can be developed. The numerical procedure to calculate heat generated due to the reaction can be summarized as follows:

i) By the time $t = t_z$, the inihibitor will be consumed. The induction time is when all the (available) inhibitor has been consumed with initiator. To determine the induction time t_z, check if

$$2f(I_o - I) = 2fI_o(1 - e^{-\int_0^t k_d dt}) \geq qZ_o. \tag{6}$$

ii) If the above condition (6) is achieved, then the induction time and the concentration of the residual initiator can be determined by

$$2fI_o(1 - e^{-\int_0^{t_z} k_d dt}) = qZ_o \tag{7}$$

and

$$I_r = I_o e^{-\int_0^{t_z} k_d dt}, \tag{8}$$

respectively.

iii) After the induction time, the conversion rate is determined by the equation (4). Also, the reaction propagates and generates heat when $t > t_z$

$$\dot{r} = H_R M_o \frac{d\alpha}{dt}, \tag{9}$$

where H_R is heat of reaction and M_o, the initial concentration of monomer.

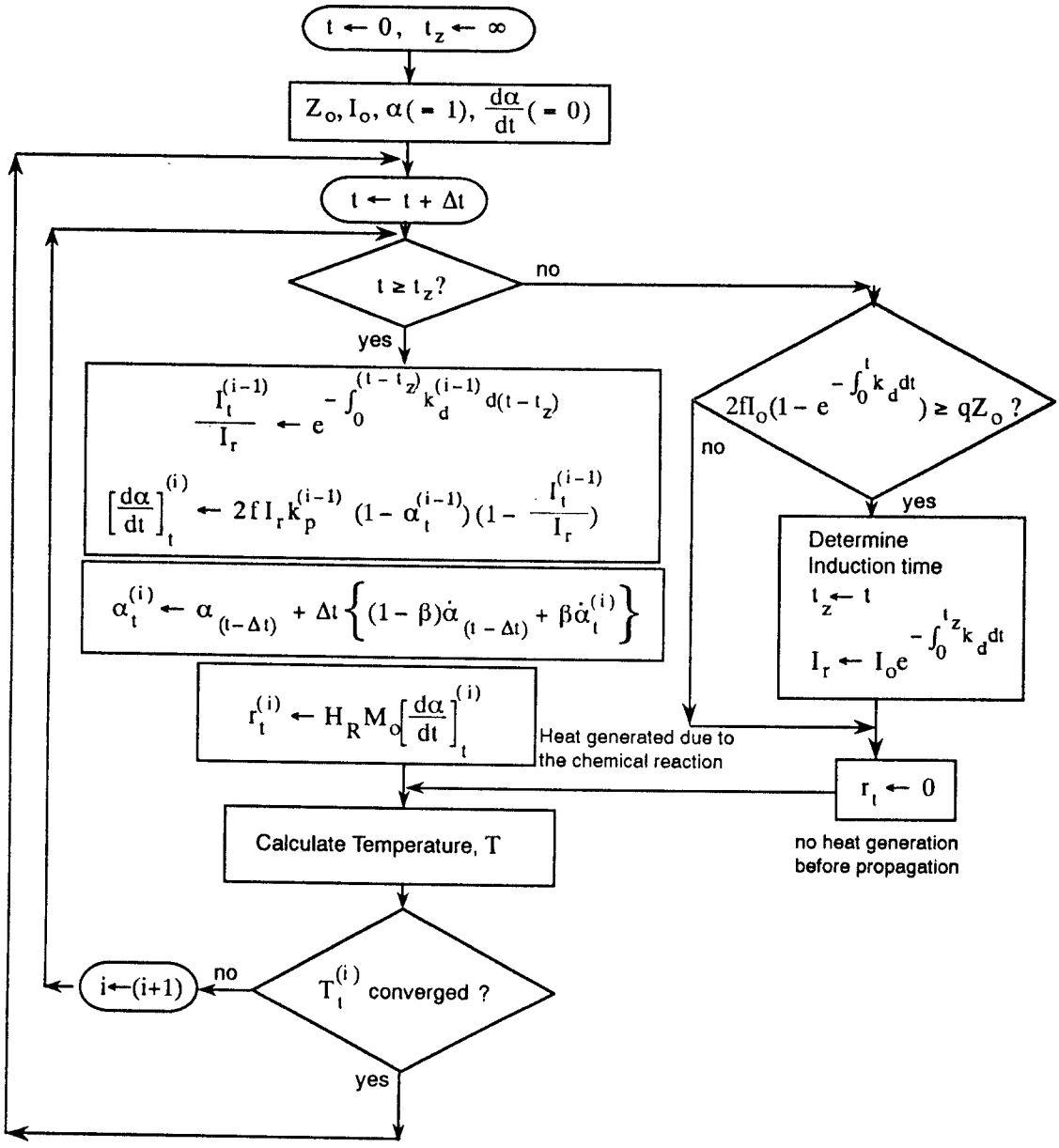

Fig. 3 Flow chart for curing combined in heat transfer analysis.

These procedures are summarized in Fig. 3. The heat generated during the chemical reaction is added into the heat balance equation during the heat transfer analysis.

IV. THEORETICAL COMPUTATION

IV.1 Finite element formulation for deformation

In large deformation problems, the assumption that elastic components of strain can be neglected is widely accepted and gives practical solutions to the problems in industry. The problems are limited to quasi-static and infinitesimal deformation based on the rigid-plastic approach in the formulation. The inertial effects, body forces, and changes in geometry due to deformation are neglected. Then the equilibrium equations and boundary conditions are written as

$$\sigma_{ij,j} = 0 \tag{10}$$

$$\left.\begin{aligned} v_i &= \bar{v}_i \quad \text{on} \quad S_U \\ \sigma_{ij} n_j &= \bar{t}_i \quad \text{on} \quad S_F \end{aligned}\right\} S_U + S_F = S_{Total} \tag{11}$$

The flow-rule (constitutive equations) can describe the relationship between the stresses and the strain-rates in the plastically deforming body as follows:

$$\dot{\varepsilon}_{ij} = \frac{3}{2}\frac{\bar{\dot{\varepsilon}}}{\bar{\sigma}}\sigma'_{ij} , \tag{12}$$

where $\bar{\dot{\varepsilon}}^p = \left(\frac{2}{3}\dot{\varepsilon}^p_{ij}\dot{\varepsilon}^p_{ij}\right)^{\frac{1}{2}}$ and $\bar{\sigma} = \left(\frac{3}{2}\sigma'_{ij}\sigma'_{ij}\right)^{\frac{1}{2}}$.

The weak form of the boundary value problem including boundary conditions and the constraint of incompressibility is

$$\int_V \sigma'_{ij}\ \delta\dot{\varepsilon}_{ij} dV - \int_{S_F} \bar{t}_i \delta v_i dS + \int_V k\,\dot{\varepsilon}_{kk}\delta\dot{\varepsilon}_{kk} dV = 0 , \tag{13}$$

where k is a penalty constant (a very large positive constant). The boundary value problem in integral form can be readily discretized by taking the velocities as the field variables.[25] Velocities and their variations are discretized and approximated as

$$\underline{v} = \underline{N}\,\hat{\underline{v}} \quad \text{and} \quad \delta\underline{v} = \underline{N}\,\delta\hat{\underline{v}} , \tag{14}$$

where **N** is a matrix of the shape functions and $\hat{v}$, the nodal values of velocity. By substituting the interpolated approximate velocity field given by equations (14) into the integral form of the boundary value problem, an error is induced which can be minimized by use of Galerkin's method where the shape functions in the matrix **N** are used as test functions. Substitution of the above equations (14) and the relationship of

strain rate-velocity (compatibility equation), $\dot{\varepsilon}_{ij} = \frac{1}{2}(v_{i,j} + v_{j,i})$ into (13) yields an integral equation in the matrix-vector form instead of the tensor notation, i.e.,

$$\int_V \frac{2}{3}\frac{\bar{\sigma}}{\hat{\dot{\varepsilon}}}\dot{\underline{\varepsilon}}^T \underline{D}\,\delta\dot{\underline{\varepsilon}}\,dV + \int_V k(\underline{c}^T\dot{\underline{\varepsilon}})^T\delta(\underline{c}^T\dot{\underline{\varepsilon}})dV - \int_{S_F}\underline{t}^T\delta\underline{v}\,dS$$
$$- \left\{\int_V \frac{2}{3}\frac{\bar{\sigma}}{\hat{\dot{\varepsilon}}}\hat{\underline{v}}^T\underline{B}^T\underline{D}\,\underline{B}\,dV + \int_V k\,\hat{\underline{v}}^T\underline{B}^T\underline{c}\,\underline{c}^T\underline{B}\,dV - \int_{S_F}\underline{t}^T\underline{N}\,dS\right\}\delta\hat{\underline{v}} = 0\,, \quad (15)$$

where $\dot{\underline{\varepsilon}} = \underline{A}\underline{v} = \underline{A}\underline{N}\,\hat{\underline{v}} = \underline{B}\hat{\underline{v}}$, $\dot{\varepsilon}_{kk} = \dot{\varepsilon}_{11} + \dot{\varepsilon}_{22} + \dot{\varepsilon}_{33} = \underline{c}^T\dot{\underline{\varepsilon}}$, and $\dot{\varepsilon}_{ij}\dot{\varepsilon}_{ij} = \dot{\underline{\varepsilon}}^T\underline{D}\,\dot{\underline{\varepsilon}}$, are applied for discretization of the strain-rate field. Since $\delta\hat{v}$ is arbitrary in equation (15), we obtain a nonlinear equations system such as

$$\Phi(\hat{\underline{v}}) = \int_V \frac{2}{3}\frac{\bar{\sigma}}{\hat{\dot{\varepsilon}}}\underline{B}^T\underline{D}\,\underline{B}\,dV\,\hat{\underline{v}} + \int_V k\,\underline{B}^T\underline{c}\,\underline{c}^T\underline{B}\,dV\hat{\underline{v}} - \int_{S_F}\underline{t}^T\underline{N}\,dS = 0\,. \quad (16)$$

Deformation of a material in a forming process is controlled only through the contact between the material and the rigid tools. Since the stiffness matrix obtained after linearizing equation (16) includes the first derivative of the friction term, a modelling having smooth variation in the relative direction is desirable. Chen and Kobayashi[26] proposed a velocity-dependent frictional stress, expressed by

$$\mathbf{f} = -mk\left(\frac{2}{\pi}\tan^{-1}\left(\frac{|\mathbf{v}_r|}{a}\right)\right)\frac{\mathbf{v}_r}{|\mathbf{v}_r|}\,, \quad (17)$$

where $\mathbf{v}_r$ is the relative velocity, a, a small constant of order 10^{-4}-10^{-5}, m, the friction factor, and k, the yield shear stress. The relative velocity is approximated by

$$\mathbf{v}_r = \tilde{N}(\hat{\mathbf{v}} - \mathbf{v}_{tool})\,, \quad (18)$$

where $\tilde{N}$ is a matrix of shape functions of the relative velocities and $\mathbf{v}_{tool}$ is the velocity of the tool.

IV.2 Finite element formulation for heat transfer

The energy balance equation for heat transfer analysis is expressed as

$$(k_i T_{,i})_{,i} - \rho C_p\dot{T} + \dot{r} = 0 \quad (19)$$

,where T is temperature, $\dot{T}$, temperature rate, k_i, the thermal conductivity in the i-direction, ρ, the density, C_p, the specific heat at constant pressure, and $\dot{r}$, the rate of heat generation per unit volume. The rate of heat generation is due to the plastic work and the chemical reaction. The associate boundary conditions are

$$T = T^* \quad \text{on} \quad S_T\,,$$
$$q_n = q_n^* = k_n\left(\frac{\partial T}{\partial n}\right)^* \quad \text{on} \quad S_q\,. \quad (20)$$

The equation (19) can be solved in a weak form with incorporating the boundary conditions (20) into the same integral. As in the deformation formulation, the following integral equation should be satisfied.

$$\int_V [k_i T_{,i}\, \delta T_{,i}\, dV + \int_V \rho C_p \dot{T} \delta T\, dV - \int_V \dot{r} \delta T\, dV - \int_{S_q} q_n^* \delta T\, dS = 0 \ . \qquad (21)$$

In the finite element discretization, the temperature and the temperature gradient fields are represented by the nodal temperature vector, $\hat{\underline{T}}$, through the shape function vector and the matrix $\underline{\mathbf{M}} = [\frac{\partial \underline{\mathbf{N}}}{\partial x}, \frac{\partial \underline{\mathbf{N}}}{\partial y}, \frac{\partial \underline{\mathbf{N}}}{\partial z}]$ as in the following.

$$T = \underline{\mathbf{N}} \hat{\underline{T}} \quad \text{and} \quad T_{,i} = \underline{\mathbf{M}} \hat{\underline{T}} \ . \qquad (22)$$

By using equations (22), equation (21) can be readily discretized as follows:

$$\delta \hat{\underline{T}}^T \{ \int_V [k_1 \underline{\mathbf{M}}^T \underline{\mathbf{M}}\, dV\, \hat{\underline{T}} + \int_V \rho C_p \underline{\mathbf{N}}^T \underline{\mathbf{N}}\, dV\, \dot{\hat{\underline{T}}} - \int_V \dot{r} \underline{\mathbf{N}}^T dV - \int_{S_q} q_n^* \underline{\mathbf{N}}^T dS \} = 0 \ . \qquad (23)$$

The heat flux on the boundary surface, q_n^*, can be categorized into two types, the heat flux on the free surface and the heat flux on the mold contacting surface. For a free surface, the heat flux is due to the radiation and the convection,

$$q_n = \sigma \varepsilon (T_e^4 - T_s^4) + h(T_e - T_s) \qquad (24)$$

,where σ is the Stephen-Boltzman constant, ε, the emissivity, h, the convection heat transfer coefficient, T_e, the environment temperature, T_s, the surface temperature. For a mold contacting surface, the heat flux is due to the convection and the friction at the mold-workpiece interface,

$$q_n = h_{lub}(T_m - T_s) + q_f \ , \qquad (25)$$

where h_{lub} is the heat transfer coefficient between mold and workpiece, T_m, the mold surface temperature, q_f, the heat generation rate due to friction.

An implicit one-step method used in the time integration in equation (23) is

$$T_t = T_{t-\Delta t} + \Delta t \{(1-\beta)\dot{T}_{t-\Delta t} + \beta \dot{T}_t\}. \qquad (26)$$

Rearranging the above equation, the temperature rate can be determined as,

$$\dot{T}_t = \frac{1}{\beta \Delta t} T_t - \bar{T} \quad \text{and} \quad \bar{T} = -\frac{1}{\beta \Delta t} T_{t-\Delta t} - (\frac{1-\beta}{\beta}) \dot{T}_{t-\Delta t} . \qquad (27)$$

Substituting equations (24), (25), and (27) into equations (23) yields

$$[\underline{\mathbf{K}} + \frac{1}{\beta \Delta t} \underline{\mathbf{C}} + \underline{\mathbf{Q}}] \hat{\underline{T}} = \underline{\mathbf{r}} + \underline{\mathbf{q}}_1 + \underline{\mathbf{q}}_2 + \underline{\mathbf{C}} \bar{\underline{T}} \qquad (28)$$

where

$$\underline{K} = \int_V [k_1 \underline{M}^T \underline{M}\, dV \quad , \quad \underline{C} = \int_V \rho C_p \underline{N}^T \underline{N}\, dV \quad , \quad \underline{\Omega} = \int_{S_q} < h, h_{lub} > \underline{N}^T \underline{N} dS \quad ,$$

$$\underline{r} = \int_V r \underline{N}^T dV \quad , \quad \underline{q}_1 = \int_{S_q} < \sigma\varepsilon(T_e^4 - T_s^4), q_f > \underline{N}^T dS \quad , \text{ and}$$

$$\underline{q}_2 = \int_{S_q} < h, h_{lub} > \underline{N}^T T_e dS \quad .$$

Overall numerical procedures including deformation, heat transfer, and chemical reaction are summarized in Fig. 4.

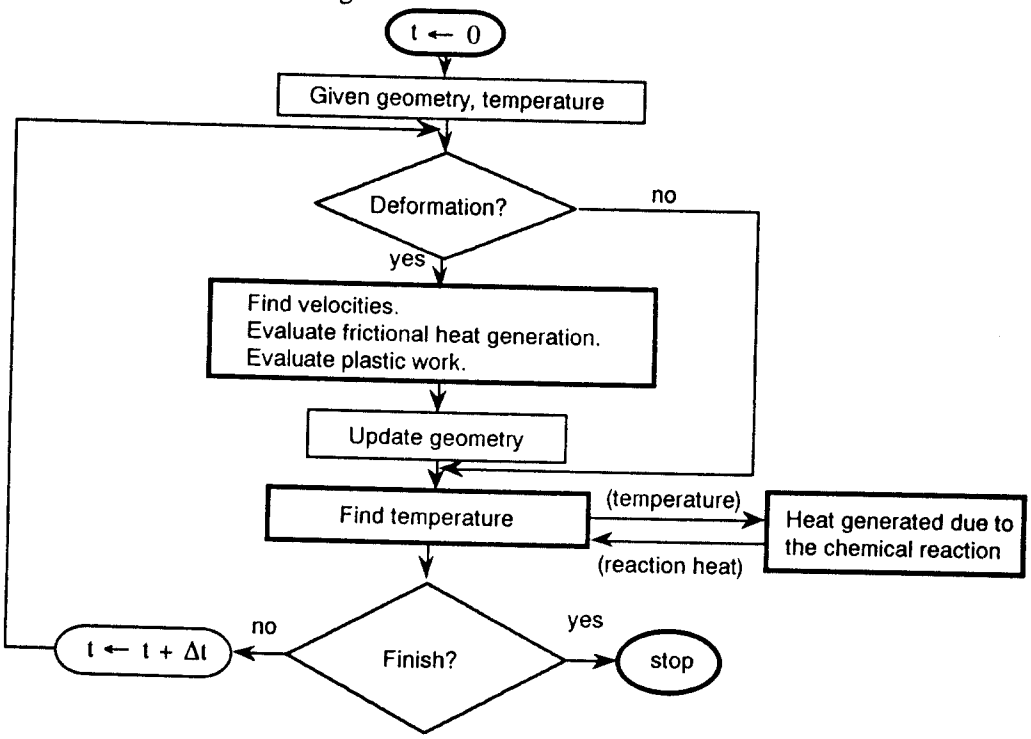

Fig. 4 Flow chart for overall procedure.

IV.3 Computational conditions

The detailed recipe for the SMC used in this study is listed in Table 1. T-butyl perbenzoate (TBPB) is a high temperature initiator, which is widely used in most commercial SMC compounds. In general, the reaction starts after an induction time and passes through a maximum rate, then drops down to zero rate. The thermal properties of SMC compounds used in this study are summarized in Tables 2. All the data used in this study were found in the literature[16]. The processing parameters used in the computation is as follows:

Mold temperature: 130 and 150 °C,

Closing speed: 1.0 and 10 in./min.,

Dwelling time: 10 seconds (if considered),

The material properties of SMC used in the simulation is as follows:

$$\tau_o = 0.05321\, e^{3010.9(\frac{1}{T} - \frac{1}{295.15})}, \quad C = 2.6159\, e^{9021.7(\frac{1}{T} - \frac{1}{295.15})},$$

$$\bar{\sigma} = 1.732\tau_o + 1.8C\dot{\bar{\varepsilon}}^{0.07}, \quad \frac{\partial \bar{\sigma}}{\partial \dot{\bar{\varepsilon}}} = 1.8C(0.07)\,\dot{\bar{\varepsilon}}^{(0.07-1)}$$

VI. COMPUTATIONAL RESULTS

Figure 5 shows experimental setups used by Fan et al.[16] The grid distortions during the mold filling stage obtained by applying the thermo-viscoplastic finite element algorithms, is shown in Fig. 6. Two different dwelling conditions are simulated. In Fig. 6 (a), when the SMC charge are put on the mold and dwelled for 10 sec, the temperature distributions become asymmetric and hence the flow on the lower mold side is faster than the upper side.

Table 1. Recipe for the SMC (parts by weight).[16]

Unsaturated polyester	33.5
Styrene	48.5
Low profile additive	18.0
$CaCO_3$	200.0
T-butyl perbenzoate (TBPB)	1.25
1" long glass fiber strand	28.0

Table 2. Thermal and Kinetic Data of SMC Used in This Study [16]

	SMC paste	SMC
ρ(g/cc)	1.85	1.89
C_p(cal/g°C)	0.267	0.258
k(cal/cm-s-°C)	0.00088	0.00092
h(cal/cm^2-s-°C)	0.0119	0.0119
H_R (cal/g)	32.15	29.40
A_d (app unit)	7.82×10^{13}	7.82×10^{13}
E_d (kcal/g-mole)	31.90	31.90
A_p (app unit)	1.71×10^{13}	1.71×10^{13}
E_p (kcal/g-mole)	16.71	16.71
$2fI_0$ (mole/g-SMC)	7.90×10^{-5}	7.32×10^{-5}

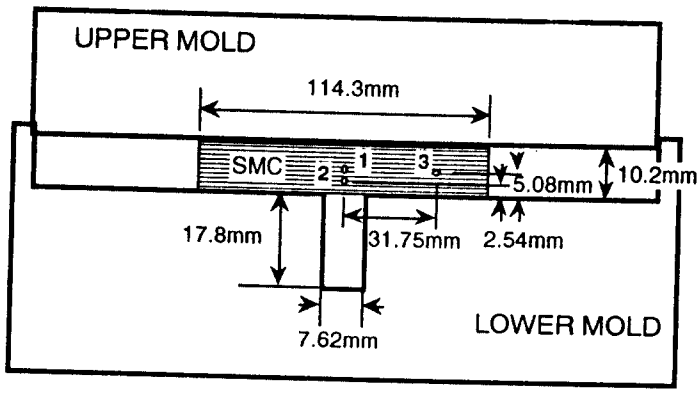

Fig. 5 Schematic of mold set-up showing the locations of the thermocouples.

Figure 7 shows computed and measured temperature profiles of SMC molding at 130 °C and a closing speed of 5 in./min. The peak of the temperature is an indication of the cure reaction. Even though the cure reaction is simulated faster at the location 3 and the temperature is lower at the location 1 compared to the experiments, the variations of temperature with respect to time shows quite a good agreement each other. Figure 8 shows similar results at higher molding temperature, 150 °C. In the figure, both the cure time and peak temperature agree with the experiments well. In general, it should be noted that the material in the center of the rib substructure cures slower than that in the flat plate part. When compared with Fig. 7, Fig. 8 shows that SMC cures much faster at 150 °C than at 130 °C.

Figure 9 and 10 show the simulated temperature distributions in the workpiece during curing process. In the earlier time, the rightend part of SMC charge becomes hottest because of the largest surface area for heat transfer. Since the T-slot is completely filled after the mold filling in the horizontal part, the temperature at the bottom is lower that that of the rightend part. In the figures, the cure patterns in the workpiece can be estimated.

Figure 11 shows the induction time contour from the cure simulation including mold filling. The area with the shortest induction time (i.e., earliest reaction) are at the rightend part and the bottom corners of the rib because of the largest surface area for heat transfer. The area with the longest induction time appears in the middle region of the rib. This is because of the long distance for heat conduction and the material flow to fill the rib before heat can be conducted into that area from the mold surface. Since the no-dwelling conditions are applied to the simulattion, the simulated cure pattern looks symmetric. In the actual SMC compression molding, the heat transfer from the

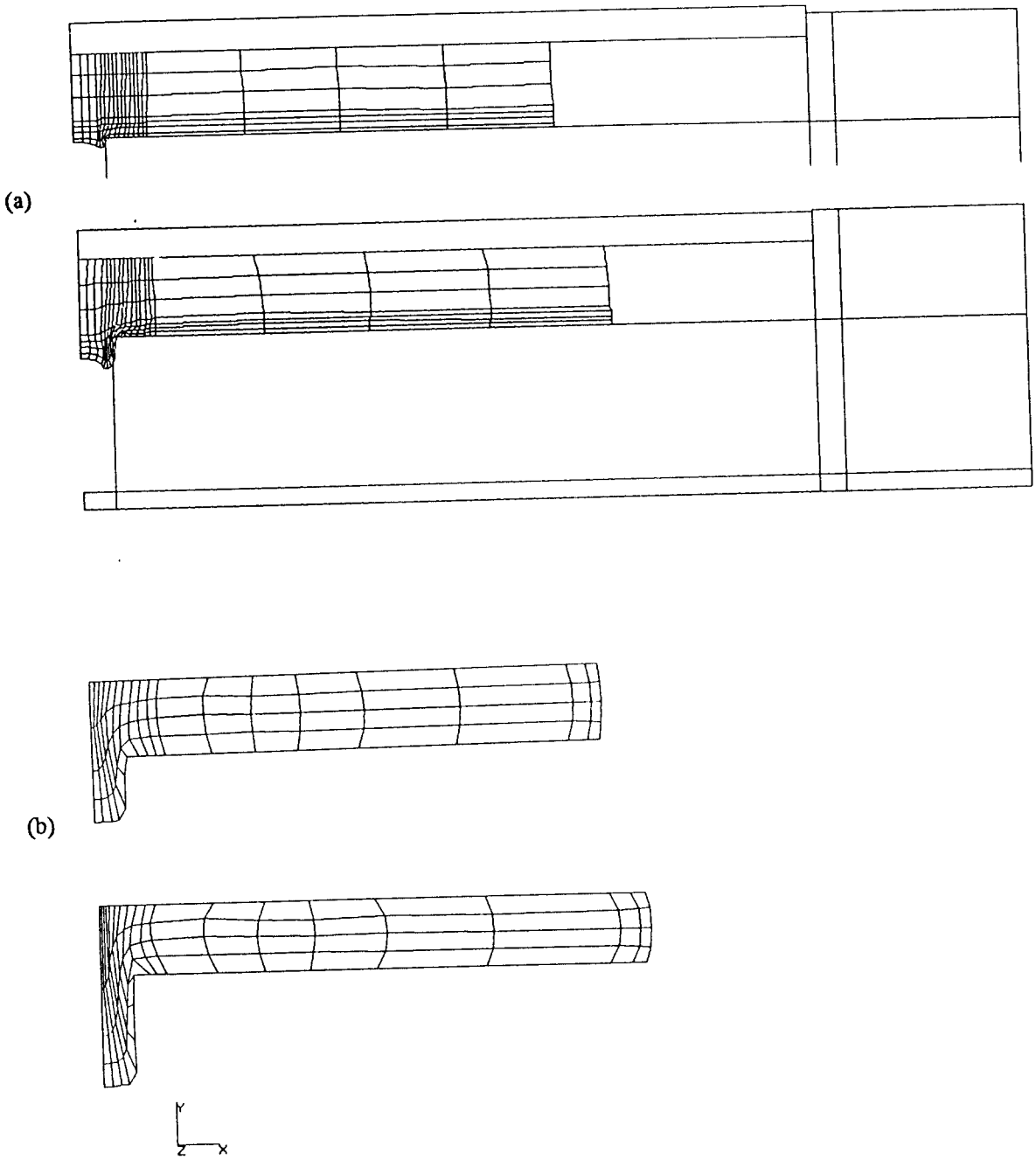

Fig. 6 Grid distortions during mold filling:
(a) dwelling time is given and (b) no dwelling.

(a)

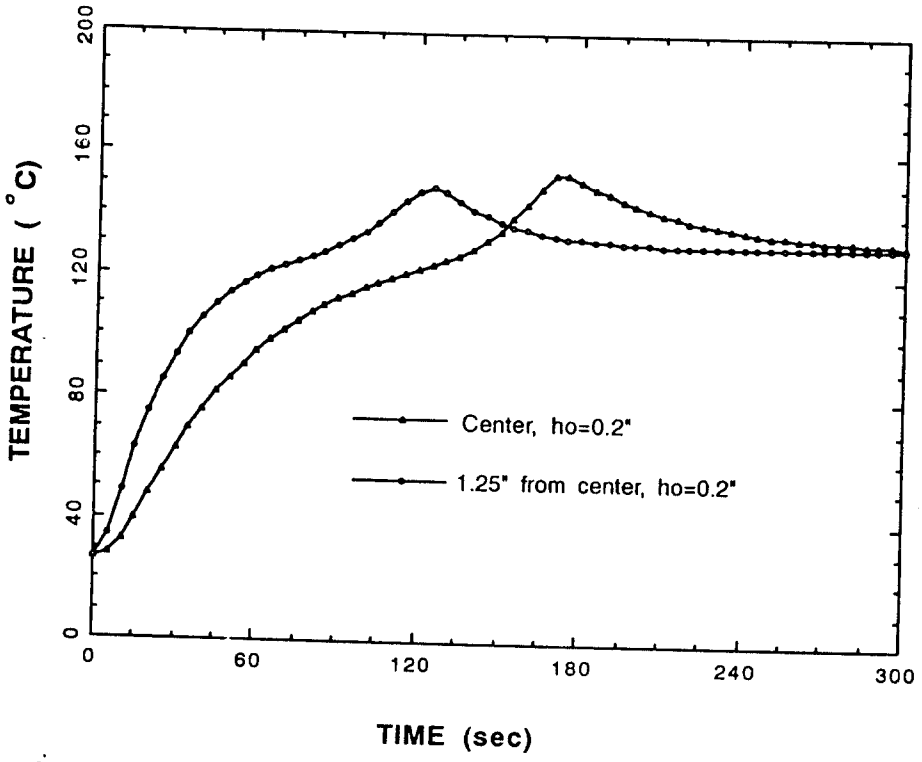

(b)

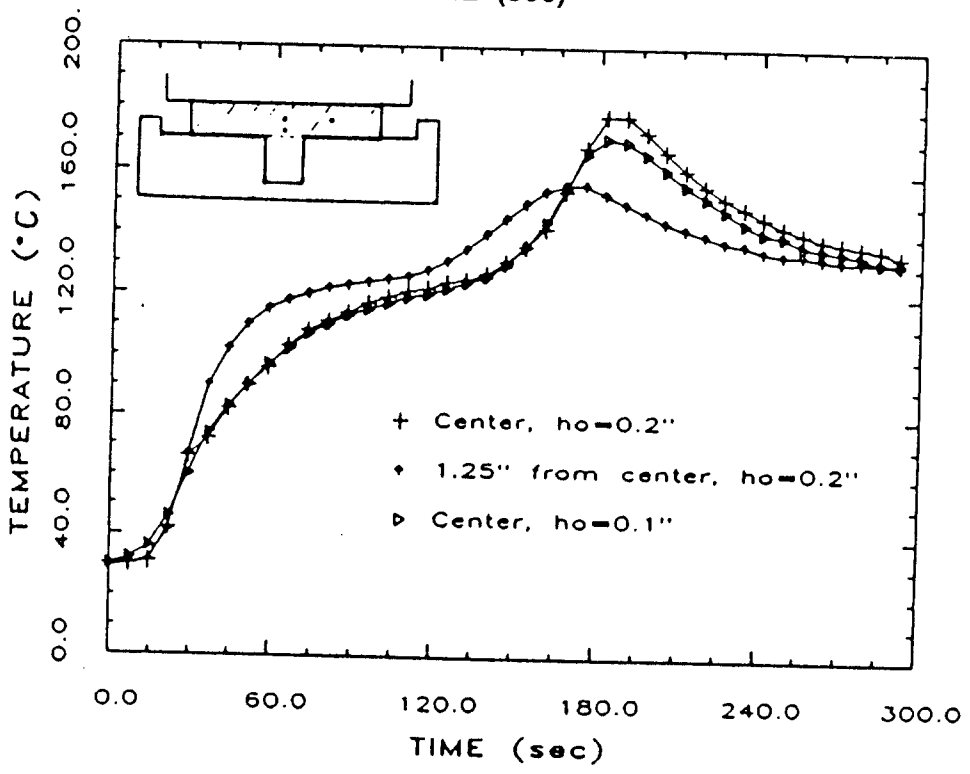

Fig. 7 Temperature variations in SMC molding, T_m=130 °C: (a) computed and (b) measured [16].

(a)

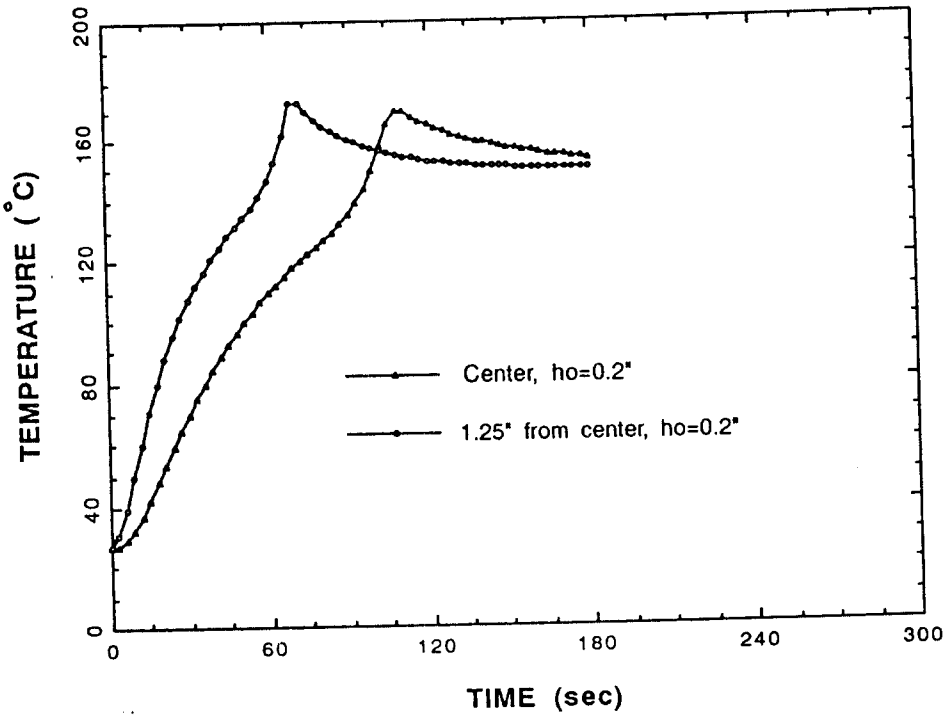

(b)

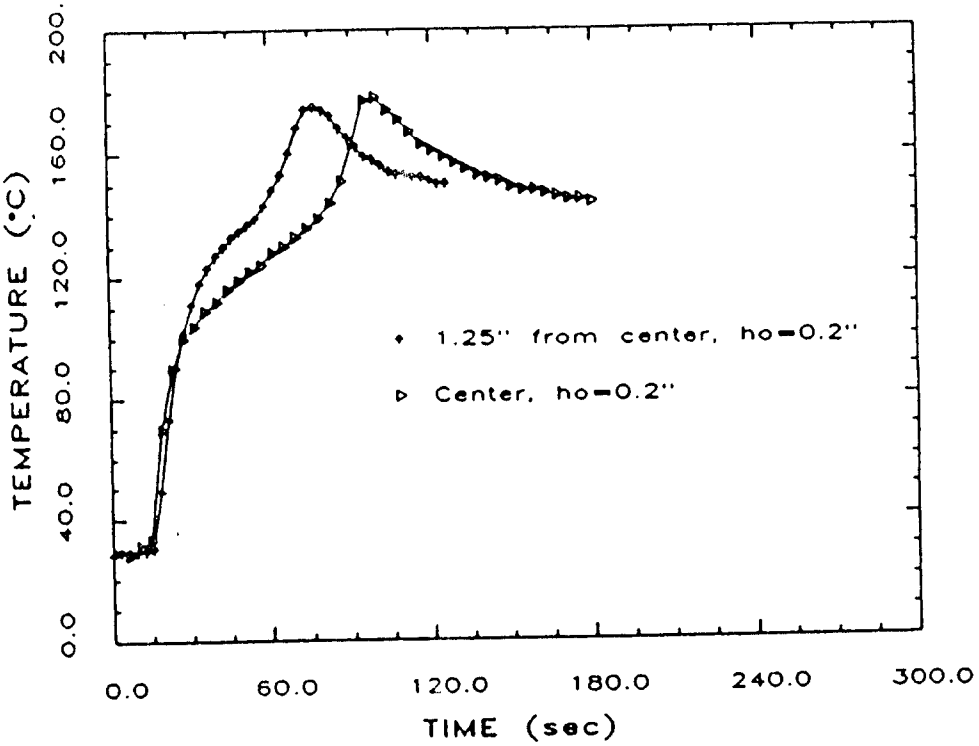

Fig. 8 Temperature variations in SMC molding, T_m=150 °C: (a) computed and (b) measured[16]

bottom mold to the charge during the dwelling would generate an asymmetric cure pattern through the part. In other words, the material near the bottom surface tends to react earlier than that at other locations.

VII. CONSLUSIONS AND REMARKS

The goal of the process analysis is to provide sufficient information to produce SMC parts from fast-cure resins without any surface defects and molding problems. In this study, an integrated approach to analyze the SMC molding process has been demonstrated.

In the flow and the cure studies, the developed analysis methods were verified with experiments. Based on the technology developed, we can further combine with other analysis techniques for optimal mold, process, and compound design. The techniques developed for T-shape parts can be extended to investigate other part geometries, such as "π" shape for the simulation of multiple-rib structures, or "L" shape for the simulation of the parts with side walls.

Further research in the following areas should be done in order to analyze the SMC molding process and to investigate surface defects:

1. The formation of sink mark is attributed to the anisotropic flow and non-uniform cure of compounds near the intersection area of the substructure. A closer study on the fiber orientations and a realistic modeling of fiber distributions and their effects on the material flow should be performed.

2. The effects of polymerization on the flow properties should be considered during the process simulation.

3. In order to expect the amount of shrinkage, thermal expansion/contraction algorithm may be included in the analysis.

References

1 R.J. Silva-Neito, B. C. Fisher, and A. W. Birley, "Rheological Characterization of Unsaturated Polyester Resin Sheet Molding Compound," S.P.I. Conference Proceedings, Sec 2-E, 1980.

2 S. Davis and C. L. Tucker, "Experimental Rheology of Glass Fiber/Polyester Sheet Molding Compound," SPE ANTEC Tech. Papers, 524, 1988.

3 L. J. Lee, L. F. Marker and R. M. Griffith, "The Rheology and Mold Flow of Polyester Sheet Molding Compound," Polym. Composites, 2, 209, 1980.

4 S. J. Lee, M. M. Denn, M. J. Crochet and A. B. Metzner, "Compressive Flow Between Parallel Disks: 1. Newtonian Fluid with a Transverse Viscosity Gradient," J. Non-Newtonian Fluid Mechanics, 10, 3, 1982.

5 M. R. Barone and D. A. Caulk, "A Model for the Flow of a Chopped-Fiber Reinforced Polymer Compound in Compression Molding," Trans. ASME, J. Appl. Mech., 53, 361, 1986.

6 J. M. Castro and R. M. Griffith, "Kinematics and Dynamics of SMC Compression Molding," SPI Conference Proceedings, Sec 17-E, 1988.

7 L. Marker and B. Ford, "Rheology and Molding Characteristics of Glass Reinforced Sheet Molding Compounds," SPI Conference Proceedings, Sec. 16-E, 1977.
8 M. R. Barone and D. A. Caulk, "Kinematics of Flow in SMC," Polym. Composites, 6(2), 105, 1985.
9 H. T. Kau, "Molding Analysis of Sheet Molding Compound (SMC) - Flow Visualization Using Carbon Black," SPE ANTEC Tech. Papers, 27, 1987.
10 R. J. Silva-Neito, B. C. Fisher, and A. W. Birley, "Predicting Mold Flow for Unsaturated Polyester Sheet Molding Compound," RPI Tech. Papers, Sec. 7-B, 34, 1979.
11 C. L. Tucker and F. Folgar, "A Model of Compression Mold Filling," Polym. Engr. Sci., 23(2), 69, 1983.
12 C. C. Lee and C. L. Tucker, "A Simulation of Compression Molding Filling Flows," SPI Conference Proceedings, 1984.
13 T. Osswald, and C. L. Tucker, "Compression Mold Filling Simulation for Non-planar Parts Using the Finite Element/ Control Volume Approach" Paper submitted to J. Inter. Polym. Processing.
14 M. R. Barone and D. A. Caulk, "The Effect of Deformation and Thermoset Cure on Heat Conduction in Chopped-Fiber Reinforced Polyester During Compression Molding," Int. J. Heat Mass Transfer, 22, 1021, 1979.
15 C. C. Lee and C. L. Tucker, "A Simulation of Non-isothermal Compression Molding," SPE ANTEC Tech. Papers, 740, 1983.
16 J.-D. Fan, L.-J. Lee, J. Kim, and Y.-T. Im, "Process Analysis of SMC in Molds with Substructures," Report ERC/NSM-88-28, The Ohio State University, October, 1988.
17 J. Kim, "Computer Modeling and Analysis of Anisotropic Material Flow in Compression Molding of Short-fiber-reinforced Composite Material," Ph.D. dissertation, Dept. of Industrial and Systems Eng., The Ohio State University, 1990.
18 J. F. Stevenson, "Free Radical Polymerization Models for Simulating Reactive Processing," Polym. Eng. Sci., 26, 746, 1986.
19 L. J. Lee, "Curing of Compression Molded Sheet Molding Compound," Polym. Eng. Sci., 21, 483, 1981.
20 M. R. Kamal, S. Sourour, and M. Ryan, "Integrated Thermo-rheological Analysis of the Cure of Thermosets," SPE ANTEC Papers, 19, 187, 1973.
21 E. M. Herman, "Heat Transfer in Compression Molding SMC," Modern Plastics, 59, October, 1978.
22 P. K. Mallick and N. Raghupathi, "Effect of Cure Cycle on Mechanical Properties of Thick Section Fiber-Reinforced Polymer/Thermoset Moldings," Polym. Eng. Sci., 19, 774, 1979.
23 J.F. Stevenson, "Molding Simulations for Thermally Initiated Exothermic Reactions," 2nd International Conference on Reactive Processing of Polymers, 1982.
24 C. C. Lee, "Reaction and Thermal Analysis for SMC Molding in Complicated Geometries," Polymer Processing Society North American Meeting, N.Y.: Buffalo, September, 1987.
25 S. Kobayashi, S.-I. Oh, and T. Altan, "Metal Forming and the Finite-Element Method," Oxford University Press, 1989.
26 C. C. Chen and S. Kobayashi, "Rigid-plastic Finite-element Analysis of Ring Compression, Application of Numerical Methods to Forming Processes," ASME, AMD, vol. 28, pp. 163-174, 1978.

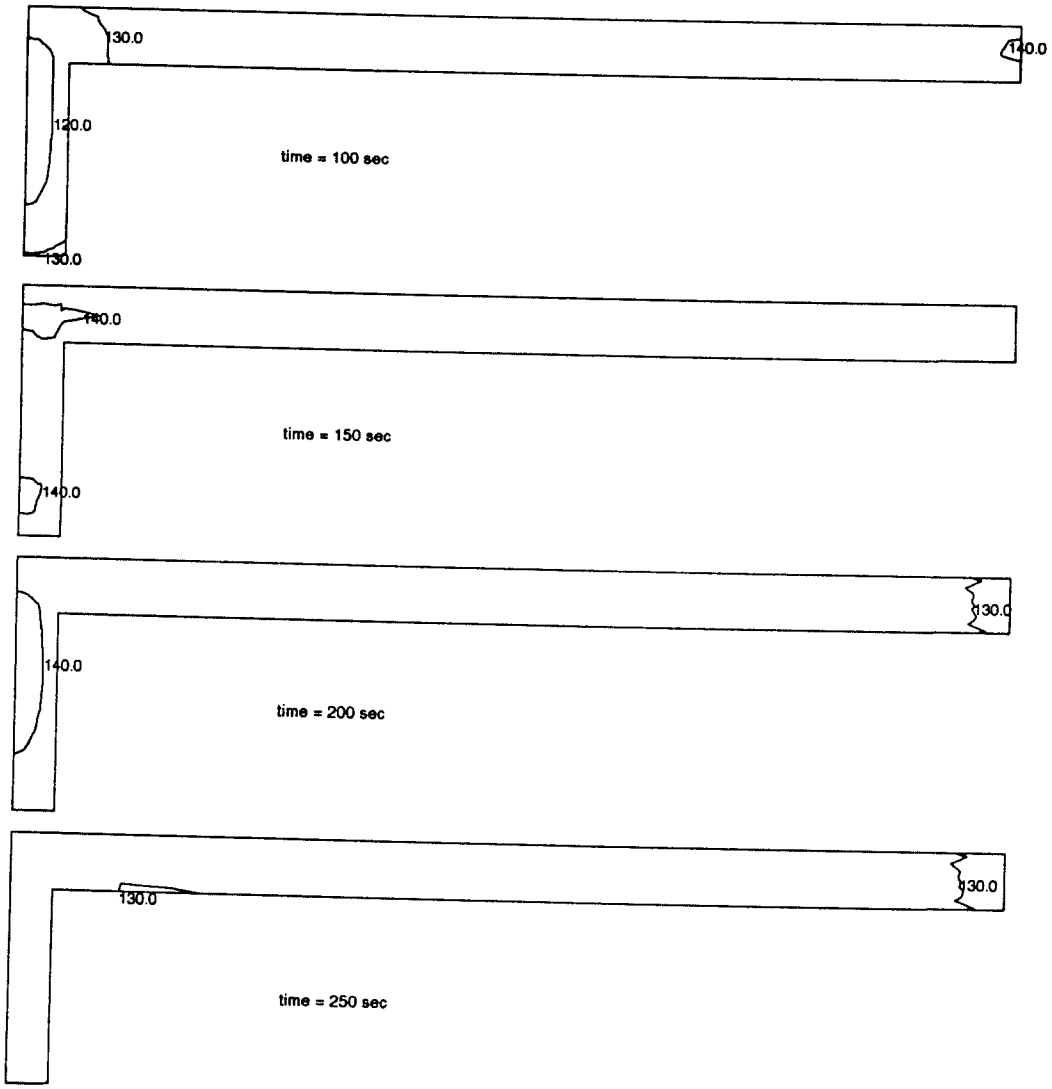

Fig. 9 Distributions of temperature, Tm=130°C

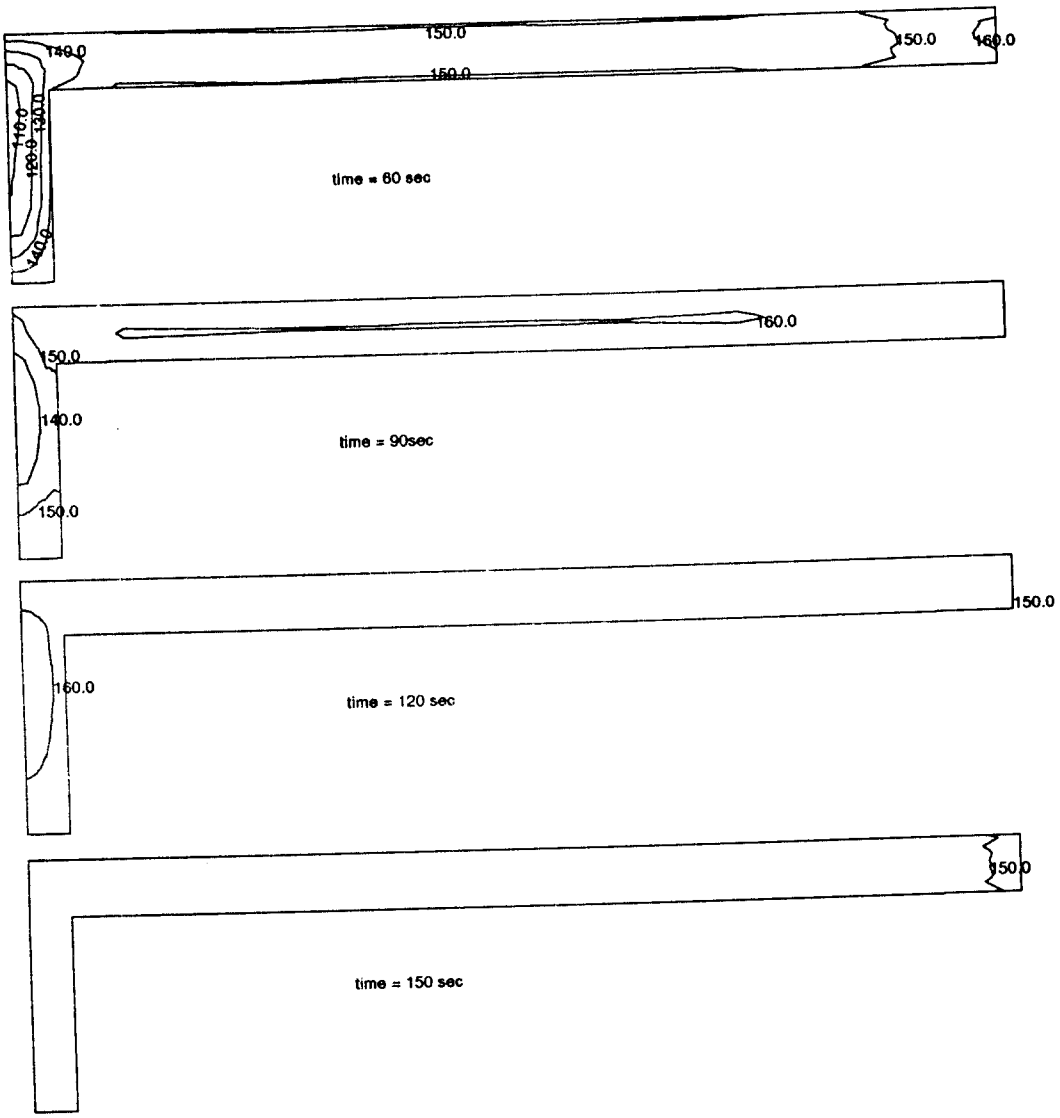

Fig. 10 Distributions of temperature, Tm=150°C

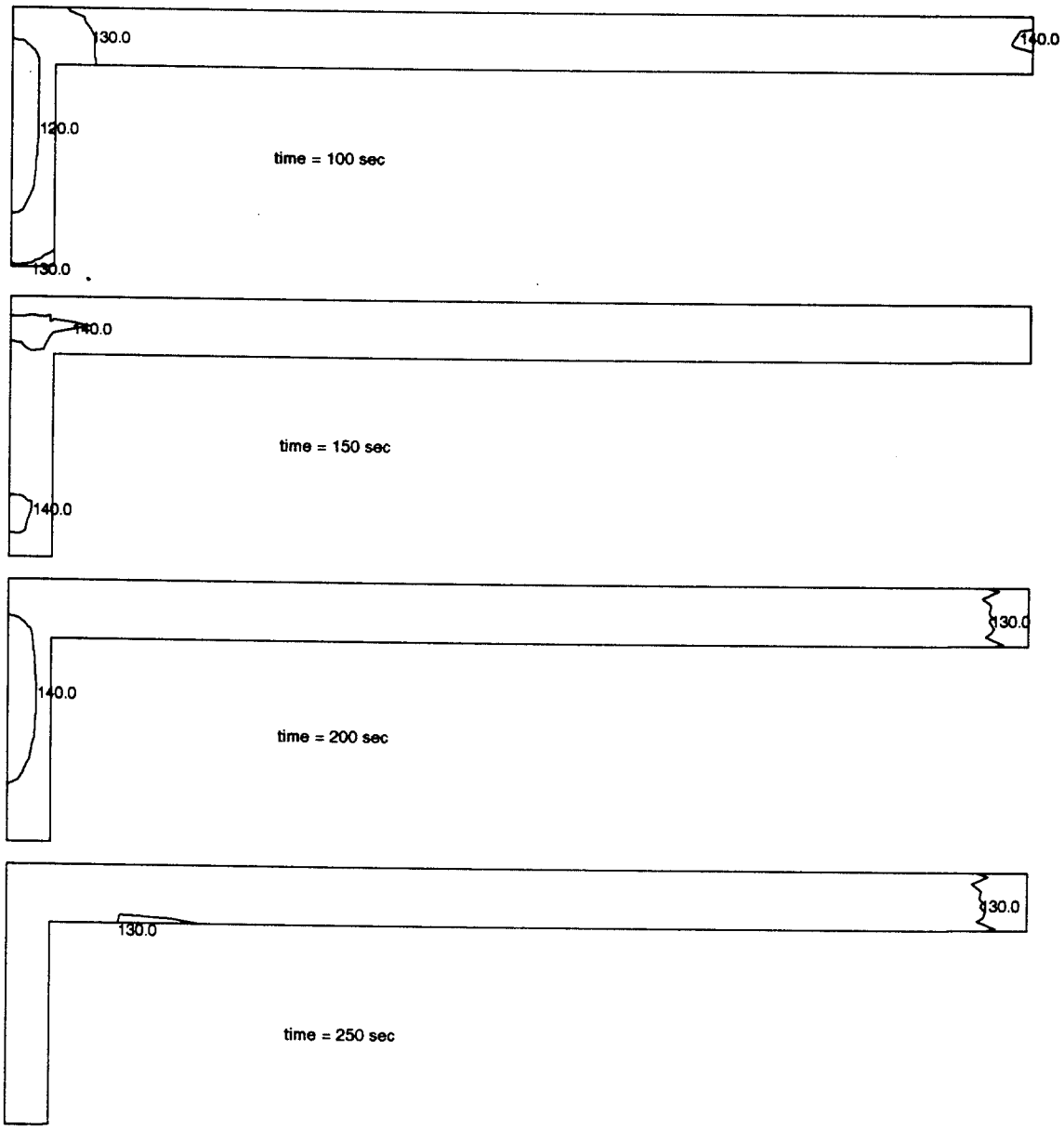

Fig. 9 Distributions of temperature, Tm=130 °C

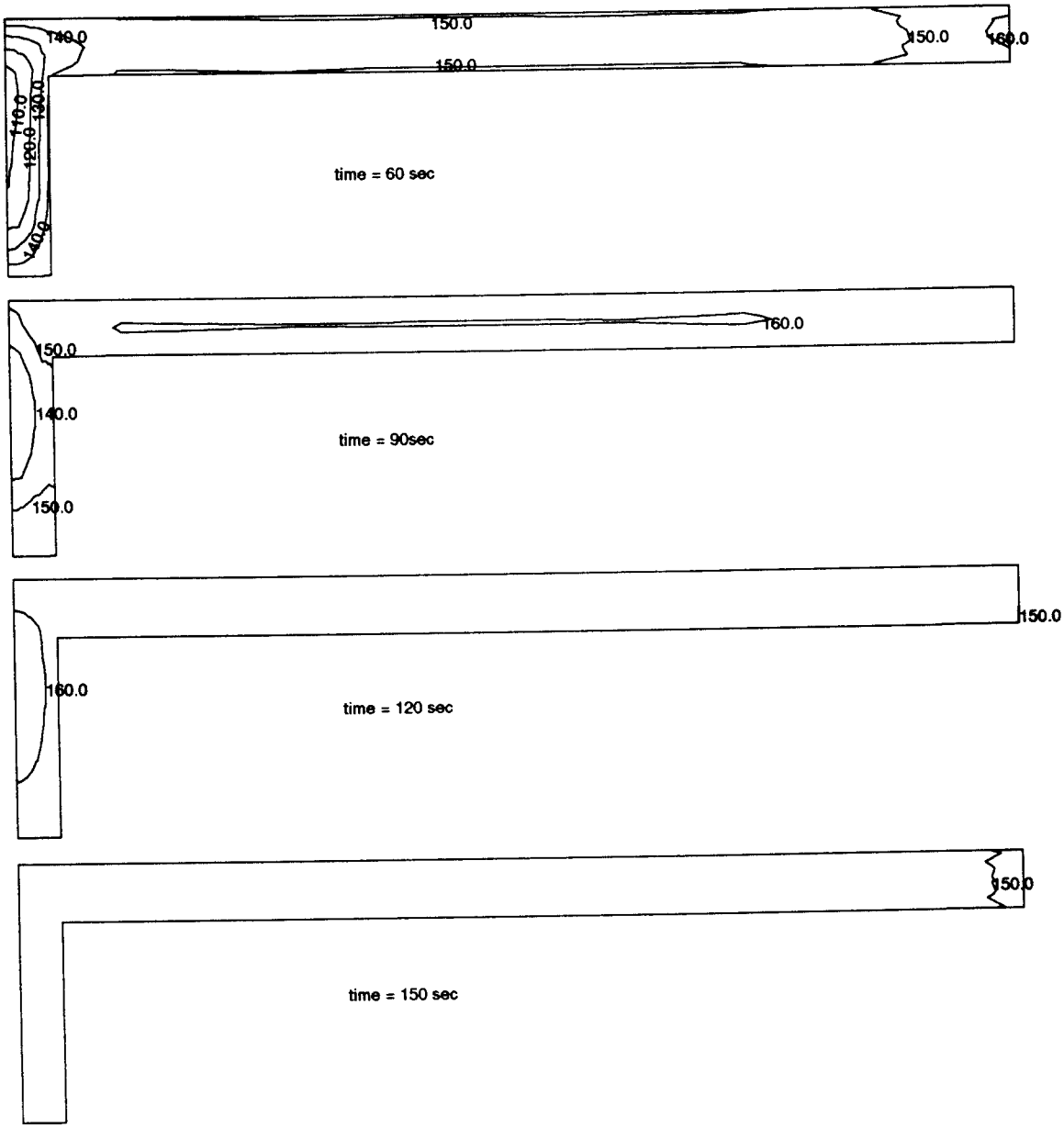

Fig. 10 Distributions of temperature, Tm=150 $^{\circ}$C

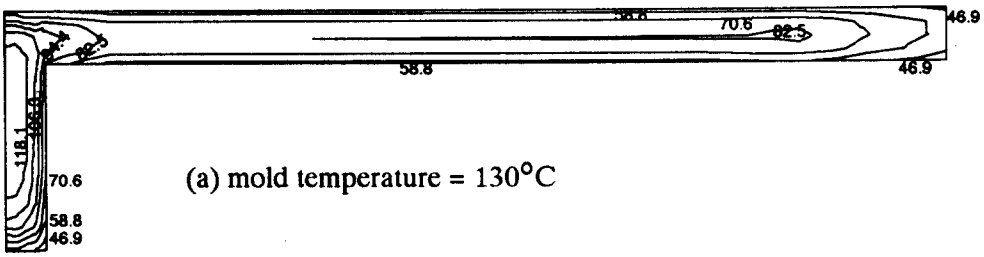

(a) mold temperature = 130°C

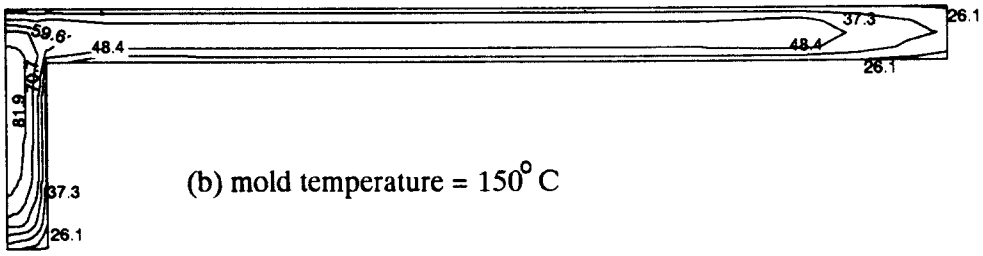

(b) mold temperature = 150° C

Fig. 11 Induction time distributions.